Strong γ-ray emission from neutron unbound states populated in β-decay: Impact on (n,γ) cross-section estimates

J.L. Tain[1,a], V. Guadilla[1], E. Valencia[1], A. Algora[1,14], A.-A. Zakari-Issoufou[2], S. Rice[3], L. Le Meur[2], J. Agramunt[1], J. Äystö[4], L. Batist[9], M. Bowry[3], J.A. Briz[2], V.M. Bui[2], R. Caballero-Folch[6], D. Cano-Ott[5], A. Cucoanes[2], V.-V. Elomaa[4], T. Eronen[4], E. Estevez[1], M. Estienne[2], M. Fallot[2], G.F. Farrelly[3], L.M. Fraile[10], E. Ganioglu[11], A.R. Garcia[5], W. Gelletly[3], B. Gómez-Hornillos[6], D. Gorelov[4], V. Gorlychev[6], J. Hakala[4], A. Jokinen[4], M.D. Jordan[1], A. Kankainen[4], V.S. Kolhinen[4], F.G. Kondev[7], J. Koponen[4], M. Lebois[12], T. Martínez[5], P. Mason[3], E. Mendoza[5], M. Monserrate[1], A. Montaner-Pizá[1], I. Moore[4], E. Nacher[13], S.E.A. Orrigo[1], H. Penttilä[4], Zs. Podolyák[3], I. Pohjalainen[4], A. Porta[2], P.H. Regan[3,15], J. Reinikainen[4], M. Reponen[4], S. Rinta-Antila[4], J. Rissanen[4], B. Rubio[1], K. Rytkönen[4], T. Shiba[2], V. Sonnenschein[4], A.A. Sonzogni[8], V. Vedia[10], A. Voss[4], and J.N. Wilson[12]

[1] Instituto de Fisica Corpuscular, CSIC - Univ. Valencia, 46980 Paterna, Spain
[2] Subatech, CNRS/IN2P3, 44307 Nantes, France
[3] University of Surrey, Department of Physics, Guilford GU2 7XH, UK
[4] University of Jyvaskyla, Department of Physics, PO Box 35, 40014 University of Jyvaskyla, Finland
[5] Centro de Investigaciones Energéticas Medioambientales y Tecnólogicas, 28040 Madrid, Spain
[6] Universitat Politecnica de Catalunya, 08028 Barcelona, Spain
[7] Nuclear Engineering Division, Argonne National Laboratory, Argonne, Illinois 60439, USA
[8] NNDC, Brookhaven National Laboratory, Upton, New York 11973, USA
[9] Petersburg Nuclear Physics Institute, 188300 Gatchina, Russia
[10] Universidad Complutense, Grupo de Física Nuclear, CEI Moncloa, 28040 Madrid, Spain
[11] Department of Physics, Istanbul University, 34134 Istanbul, Turkey
[12] Institut de Physique Nuclèaire d'Orsay, 91406 Orsay, France
[13] Instituto de Estructura de la Materia, CSIC, 28006 Madrid, Spain
[14] Institute of Nuclear Research of the Hungarian Academy of Sciences, 4026 Debrecen, Hungary
[15] National Physical Laboratory, Teddington, Middlesex, TW11 0LW, UK

Abstract. Total absorption gamma-ray spectroscopy is used to measure accurately the intensity of γ emission from neutron-unbound states populated in the β-decay of delayed-neutron emitters. From the comparison of this intensity with the intensity of neutron emission one can deduce information on the (n,γ) cross section for unstable neutron-rich nuclei of interest in r process abundance calculations. A surprisingly large γ branching was observed for a number of isotopes. The results are compared with Hauser-Feshbach calculations and discussed.

1. Introduction

The process of β-delayed neutron (βDN) emission takes place for neutron-rich nuclei when they are far enough from stability. Then the decay can populate resonances, with excitation energy E_x above the neutron separation energy S_n, that decay by neutron emission or by electromagnetic de-excitation. The branching for γ (neutron) emission is given by the ratio of γ (neutron) to total widths: $\Gamma_{\gamma,\mathrm{n}}(E_x)/\,\Gamma_{\mathrm{tot}}(E_x)$, $\Gamma_{\mathrm{tot}}(E_x) = \Gamma_\gamma(E_x) + \Gamma_n(E_x)$. Thus a measurement of the β intensity distribution preceding Γ emission $I_{\beta\gamma}(E_x)$ above S_n, and the comparison with the β intensity distribution preceding neutron emission $I_{\beta n}(E_x)$, provides information on these partial widths.

In radiative neutron capture (n, γ) reactions similar resonances are populated, although in general of a different spin-parity, and the reaction cross section $\sigma_{\mathrm{n}\gamma}$ is proportional to $\Gamma_\gamma(E_x)\Gamma_n(E_x)/\,\Gamma_{\mathrm{tot}}(E_x)$. The dependence of (n, γ) and $I_{\beta\gamma}$ on the same quantities serves as the basis for the possibility of extracting information about neutron capture cross-section for very unstable neutron-rich nuclei from β-decay studies. This is relevant to the investigation of the astrophysical r process, particularly for the calculation of elemental abundances where $\sigma_{\mathrm{n}\gamma}$ has an impact [1–3]. Lacking experimental information, cross sections for this purpose are calculated [4] using the Hauser-Feschbach formalism (HFF) based on parameterizations of average nuclear properties obtained close to the β-stability valley. Large uncertainties exist for the parameters to be used far from stability.

From the experimental point of view the main difficulty is the accurate measurement of the weak $I_{\beta\gamma}(E_x)$ above S_n. High resolution spectroscopy using HPGe detectors, due to the limited efficiency, has been able to locate only a few γ transitions in a handful of isotopes as can be deduced from the inspection of evaluated decay data bases [5]. We have shown recently [6] that total absorption

[a] e-mail: tain@ific.uv.es

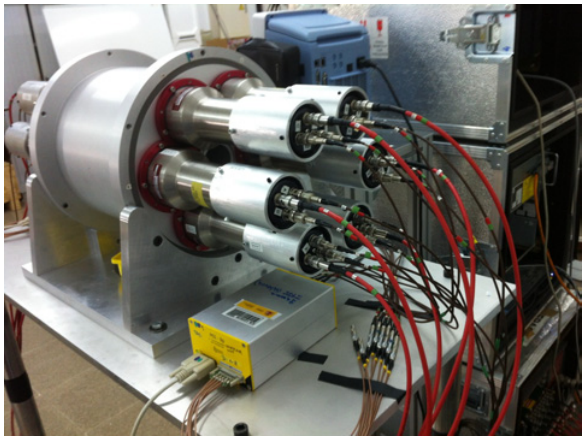

Figure 1. The compact BaF_2 total absorption spectrometer *Rocinante*.

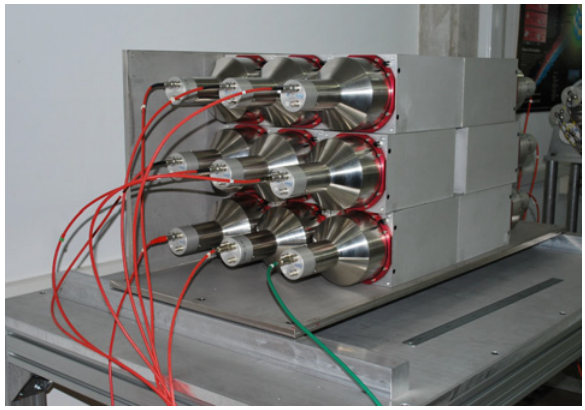

Figure 2. The modular NaI(Tl) total absorption spectrometer *DTAS*.

gamma-ray spectroscopy (TAGS) has the sensitivity and accuracy needed to provide data in the excitation energy region of interest for exotic nuclei. The TAGS technique uses 4π scintillation detectors to absorb the full energy released in the decay from which the β-intensity distribution is reconstructed by deconvolution with the spectrometer response.

2. Measurements

Two measurements have been performed up to now, each using a different spectrometer. The first measurement [6,7] was performed with *Rocinante*, a compact 12 BaF_2 crystal spectrometer with cylindrical geometry (see Fig. 1). It was the first TAGS detector with segmentation designed for β-decay studies. The segmentation allows the measurement of γ-cascade multiplicities providing strong constraints on the decay response matrix used in spectrum deconvolution. In addition the BaF_2 material was chosen in order to reduce the sensitivity of the spectrometer to β-delayed neutrons. Neutrons interact by inelastic scattering and capture reactions producing background γ-rays [8]. The second measurement was performed with *DTAS*, a modular 18 NaI(Tl) crystal spectrometer (see Fig. 2) developed for measurements at the future FAIR/NUSTAR facility [9,10]. The geometry, based on rectangular crystals, is easily reconfigurable. It allows the insertion of large ancillary detectors, for example a DSSSD implantation detector or HPGe high-resolution γ-ray detectors. The new spectrometer provides a larger detection efficiency and has a better energy resolution but is affected by one order-of-magnitude larger neutron capture background. In general background reduction and characterization is a key ingredient of the TAGS technique. We use coincidences with a β detector to eliminate the large ambient background. β signals were registered in a 1 mm thick Si detector (first experiment) or a 3 mm thick plastic scintillation detector (second experiment). In both cases the solid angle subtended by the β detector was around 30%.

Both measurements were performed at the IGISOL on-line mass separator [11] in the JYFL Cyclotron Laboratory of the University of Jyvaskyla. Fission products were produced by protons of 25 MeV in a thin uranium target inside the separator ion-guide type source. The products exiting the target are swept by a He flow into the 30 kV acceleration stage of the mass separator. A key feature of this installation is a double Penning trap system [12], located after the analyzing magnet at the end of the separator. It is used to eliminate the isobaric contamination from the fission product of interest. The purified radioactive beam was implanted on a tape at the centre of the spectrometer. The tape moved cyclically with a time period equivalent to three half-lives in order to minimize the contamination from decay descendants. In the first experiment data were obtained for ^{87,88}Br and ^{93,94}Rb, while in the second experiment we measured ^{95}Rb and ^{137,138}I. All of them are well known β-delayed neutron emitters.

The largest sources of spectrum contamination were the decay of descendants, in particular the βDN decay, and the electronic pulse pileup. The former includes the interactions of the emitted neutron with the detector, already mentioned above. Special procedures were developed [6,7] to calculate the shape and magnitude of both background components.

The spectrometer response to decays [13] was obtained by means of Geant4 [14] Monte Carlo simulations, and was calibrated with dedicated measurements. The TAGS total absorption spectrum was deconvoluted using the methodology developed by the Valencia group [15]. The decay response calculation requires assumptions on the γ-ray de-excitation pattern and we used branchings obtained from the statistical nuclear model. In addition to the reproduction of the total absorption spectrum the branching ratio assumptions were validated by comparing the measured TAGS spectra for different crystal multiplicities with simulated spectra. Systematic uncertainties in the β-intensity distribution obtained after deconvolution were thoroughly investigated. This includes uncertainties in the decay response coming from the assumptions about branching ratios and from the accuracy with which Geant4 Monte Carlo simulations can reproduce individual γ-ray and electron responses. It also includes uncertainties on background subtraction.

3. Hauser-Feshbach calculations

The Hauser-Feshbach formalism (HFF) was used to compute the average ratio of γ to total widths $\langle \Gamma_\gamma(E_x)/\,\Gamma_{\rm tot}(E_x)\rangle$. For each initial level J_i^π at E_x in the

daughter nucleus the average radiative width is obtained as the sum of the widths to each individual final level J_f^π at $E_x - E_\gamma$ in the daughter nucleus:

$$\langle\Gamma_\gamma(J_i^\pi, E_x)\rangle = \sum_f \langle\Gamma_\gamma(J_f^\pi, E_x, E_\gamma)\rangle = \frac{1}{\rho(J_i^\pi, E_x)} \sum_f \sum_{XL} E_\gamma^{2L+1} \mathrm{f}_{XL}(E_\gamma) \quad (1)$$

where $\rho(J_i^\pi, E_x)$ represents the nuclear level density (NLD) of initial levels and $\mathrm{f}_{XL}(E_\gamma)$ is the photon strength function (PSF) for transition energy E_γ. The appropriate electric or magnetic character X and multipolarity L of the transition is selected by spin and parity conservation. Likewise the average neutron width is obtained as the sum of the individual widths to the levels in the final nucleus J_f^π at $E_x - S_n - E_n$

$$\langle\Gamma_n(J_i^\pi, E_x)\rangle = \sum_f \langle\Gamma_n(J_f^\pi, E_x, E_n)\rangle = \frac{1}{2\pi\rho(J_i^\pi, E_x)} \sum_f \sum_{ls} T^{ls}(E_n) \quad (2)$$

where $T^{ls}(E_n)$ is the neutron transmission coefficient (NTC), a function of neutron energy E_n. The orbital angular momentum l and channel spin s are selected by spin and parity conservation. For the calculations we used parameters retrieved from the RIPL-3 reference input parameter library [16]. The NLD corresponds to that calculated using a Hartree-Fock-Bogoliubov (HFB) plus combinatorial approach adjusted to experimental information [17]. The PSF is obtained from Generalized Lorentzian (E1 transitions) or Lorentzian (M1 and E2 transitions) type functions using parameters from systematics. The NTC is obtained from the Optical Model (OM) using the TALYS-1.6 software package [18] with parameters taken from the so-called local parametrization of Ref. [19]. It is assumed that the actual widths for individual transitions are subject to statistical fluctuations of the Porter-Thomas (PT) type around the average values. The PT distribution, a chi-square distribution with one degree of freedom, is a very asymmetric distribution. This can introduce significant corrections [20] when calculating width ratios. In the case of reaction cross sections, for example the neutron radiative capture which depends on $\langle\Gamma_\gamma\Gamma_n/\Gamma_{\mathrm{tot}}\rangle$, the width fluctuation correction (WFC) is included in a parametric way. Several parametrizations exist and their validity is usually tested against Monte Carlo calculations. See Ref. [22] for a review of previous formulae and a new improved approximation. In this work we apply directly the MC method to the calculation of $\langle\Gamma_\gamma/\Gamma_{\mathrm{tot}}\rangle$. The MC sampling procedure is similar to that described in Ref. [21]. Level energies for each spin-parity are generated from the NLD in the daughter nucleus above the level scheme regarded as known, with spacing according to a Wigner distribution. In the final nucleus only the known level scheme is considered. For each state the corresponding Γ_γ and Γ_n to individual final states are sampled from PT distributions with the calculated average values. Then the total width is obtained by summation (Eqs. (1) and (2)), and the ratio computed. To obtain the mean value of the ratio we average all ratios for levels

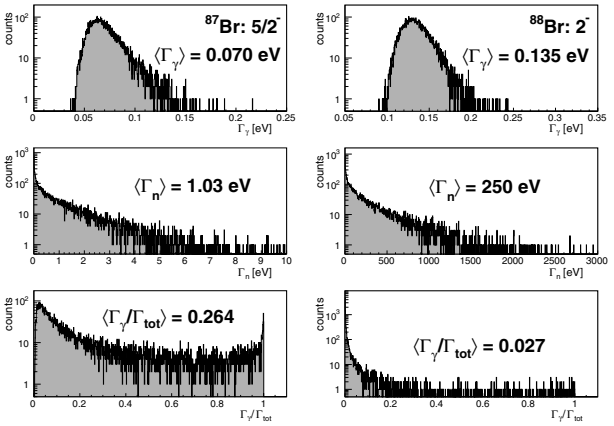

Figure 3. Results of the Monte Carlo sampling for a $5/2^-$ resonance in ^{87}Br (left panels) and a 2^- resonance in ^{88}Br (right panels). Shown are the distributions for Γ_γ (top panels), Γ_n (middle panels) and $\Gamma_\gamma/\Gamma_{\mathrm{tot}}$ (bottom panels). The average value for the different distributions is indicated.

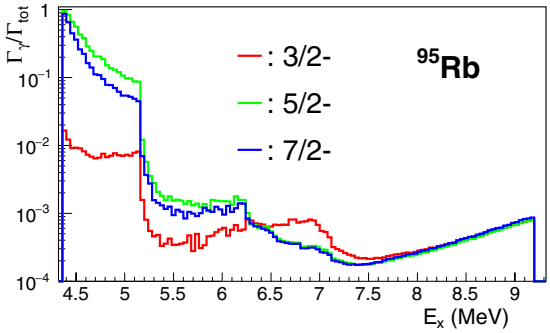

Figure 4. Calculated γ branching ratio as a function of excitation energy in the range $[S_n, Q_\beta]$ for the three spin-parity groups populated in the Gamow-Teller decay of ^{95}Rb.

of a given J_i^π within an energy bin of 40 keV. Since the level density for some of the isotopes is low, the MC sampling is repeated a sufficient number of times to give a stable numerical average. In Fig. 3 we show examples of the distribution of Γ_γ, Γ_n and $\Gamma_\gamma/\Gamma_{\mathrm{tot}}$ obtained by this procedure.

The calculations in Fig. 3 are performed for a $5/2^-$ state in ^{87}Br and for a 2^- state in ^{88}Br located in both cases 500 keV above S_n. Only the ground state in the final nucleus is available for decay by neutron emission for these states. A $5/2^-$ state in ^{87}Br requires a neutron orbital angular momentum transfer of $l = 3$ to reach the 0^+ g.s. in ^{86}Kr. Thus, the neutron emission is hindered explaining the low value of $\langle\Gamma_n\rangle$ (1 eV) and large γ branching $\langle\Gamma_\gamma/\Gamma_{\mathrm{tot}}\rangle$ (26.4%). As can be easily computed from the average values given in Fig. 3 the WFC is large: a factor of 4.2. The 2^- state in ^{88}Br can decay through the emission of an $l = 1$ neutron to the $5/2^+$ g.s. in ^{87}Kr, thus $\langle\Gamma_n\rangle$ is large (250 eV) and $\langle\Gamma_\gamma/\Gamma_{\mathrm{tot}}\rangle$ is small (2.7%). The WFC is huge in this case: a factor 50. For comparison the WFC factor calculated by the MC procedure for the ratio $\Gamma_\gamma\Gamma_n/\Gamma_{\mathrm{tot}}$, the capture cross-section, is 0.78 and 0.97 respectively. Thus, inclusion of WFC in the HFF calculation of the Γ branching is essential when comparing with β-decay experiments.

Figure 4 shows the calculated ratios $\langle\Gamma_\gamma/\Gamma_{\mathrm{tot}}\rangle$ as a function of E_x for the decay of ^{95}Rb. Assuming that the

Table 1. For each parent the spin-parity J^{π}_{GT} of Gamow-Teller states populated in the daughter nucleus, the spin-parity $J^{\pi}_{g.s.}$ of the ground state in the final nucleus, and the energy of the first excited state E^{1st}_{x} in the final nucleus are shown. J^{π}_{GT} marked as bold correspond to a neutron orbital angular momentum transfer $l > 2$.

Parent	Daughter J^{π}_{GT}	Final $J^{\pi}_{g.s.}$	Final E^{1st}_{x} [keV]
^{87}Br	$3/2^-, \mathbf{5/2^-}, \mathbf{7/2^-}$	0^+	1565
^{88}Br	$\mathbf{0^-}, 1^-, 2^-$	$5/2^+$	532
^{93}Rb	$3/2^-, \mathbf{5/2^-}, \mathbf{7/2^-}$	0^+	815
^{94}Rb	$2^-, 3^-, 4^-$	$5/2^+$	213
^{95}Rb	$3/2^-, \mathbf{5/2^-}, \mathbf{7/2^-}$	0^+	837
^{137}I	$5/2^+, \mathbf{7/2^+}, \mathbf{9/2^+}$	0^+	1313
^{138}I	$\mathbf{0^-}, 1^-, 2^-$	$7/2^-$	601

decay is of the allowed Gamow-Teller type, states with spin-parity $3/2^-$, $5/2^-$ and $7/2^-$ are populated. As can be observed for $E_x - S_n < 837$ keV, the excitation energy of the first excited 2^+ state in the final nucleus ^{94}Sr, the γ branching is large for $5/2^-$ and $7/2^-$ states. Levels populated in this energy region can decay by neutron emission to the 0^+ g.s. in ^{94}Sr only. For $5/2^-$ and $7/2^-$ states this requires an $l = 3$ transfer which is strongly retarded, one to two orders of magnitude, with respect to the $l = 1$ neutron emission for $3/2^-$ states.

4. Results and discussion

Results for ^{87,88}Br and ^{94}Rb have already been published [6]. Preliminary results exist for ^{93,95}Rb and ^{137}I, while ^{138}I is being analyzed. We summarize below the information obtained so far.

The β intensity distributions $I_{\beta\gamma}(E_x)$ obtained from the deconvolution of TAGS spectra show a sizable amount of intensity above S_n for most of the nuclei investigated. Except for ^{94}Rb, which is about 5%, the integral value $P_\gamma = \int_{S_n}^{Q_\beta} I_{\beta\gamma}(E_x)dE_x$ represents 17% to 57% of the total intensity above S_n. These surprisingly large values can be explained, as in the ^{95}Rb case above, by the population of one or more spin-parity groups of states in the daughter nucleus in a relatively large range of excitation energies above S_n that can only decay to the final nucleus g.s. with $l > 2$. See Table 1. This behaviour can be extrapolated to other β-delayed neutron emitters and can serve to identify nuclei where a strong γ emission from neutron unbound states could be expected.

The best way to make a quantitative comparison of our $I_{\beta\gamma}(E_x)$ with the HFF calculations is to combine the TAGS result with $I_{\beta n}(E_x)$, the β-intensity followed by neutron emission. Then we can use the relation

$$\frac{I_{\beta\gamma}(E_x)}{I_{\beta\gamma}(E_x) + I_{\beta n}(E_x)} = \sum_i w(J_i^\pi, E_x)\left\langle \frac{\Gamma_\gamma(J_i^\pi, E_x)}{\Gamma_{\rm tot}(J_i^\pi, E_x)} \right\rangle \quad (3)$$

where $w(J^\pi, E_x)$ are the relative weights of the different spin-parities contributing at each excitation energy in the daughter nucleus. The relative weights w can be obtained from a β-strength theoretical calculation. Lacking this information we assume that the weight is independent of energy and proportional to $(2J + 1)$ [23]. $I_{\beta n}(E_x)$ can be obtained from the β-delayed neutron energy distribution. The relation of the normalized neutron energy spectrum

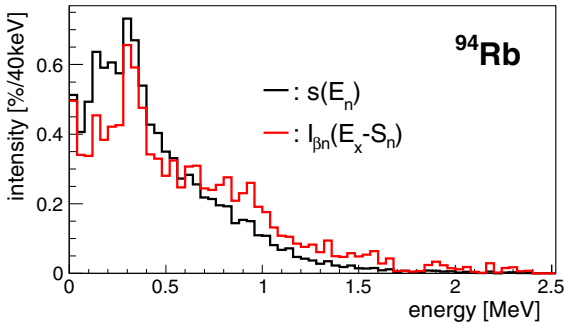

Figure 5. Normalized neutron energy spectrum for ^{94}Rb from [24] and the deduced β-intensity followed by neutron emission.

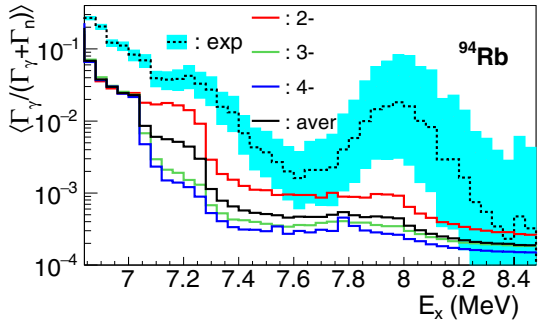

Figure 6. Experimental γ-branching (black dashed line) for neutron unbound states in ^{94}Rb decay as a function of excitation energy compared with Hauser-Feshbach estimates. The calculation is shown for the three spin-parities populated in the GT decay (red, green and blue lines) and for the weighted average (black line). The light blue area around the experiment indicates the systematic uncertainty from the TAGS analysis.

$s(E_n)$ and the intensity is given by:

$$s(E_n) = \int_{S_n}^{Q_\beta} \sum_i w(J_i^\pi, E_x)\left\langle \frac{\Gamma_n(J_i^\pi, E_x, E_n)}{\Gamma_n(J_i^\pi, E_x)} \right\rangle \times I_{\beta n}(E_x)dE_x \quad (4)$$

We have thus obtained the β-intensity followed by neutron emission by deconvolution of the neutron spectrum with the calculated neutron branching to the different levels in the final nucleus. Note that the neutron intensity to the levels in the final nucleus calculated with HFF does not necessarily agree with the observed intensities, introducing some systematic error in the deduced $I_{\beta n}(E_x)$. Neutron spectra were taken from the ENDF/B-VII.1 evaluated nuclear data base [24]. Figure 5 compares the neutron spectrum with the result of the deconvolution for the case of ^{94}Rb.

With this information it is possible to calculate the experimental γ-branching as a function of excitation energy and compare it with the theoretical estimate as is done in Fig. 6 for the decay of ^{94}Rb. This case is particularly relevant because it is the only one where the γ branching is small. This is in accord with the HFF calculation showing that neutron emission from the allowed GT states in the measured E_x range is not particularly hindered, thus $\langle\Gamma_\gamma\rangle \ll \langle\Gamma_n\rangle$. This makes the ratio $\langle\Gamma_\gamma/\Gamma_{\rm tot}\rangle$ more sensitive to the magnitude of $\langle\Gamma_\gamma\rangle$ than for the remaining nuclei. However as can be seen in Fig. 6 the calculation for all J^π is too low in comparison to the measurement. We have estimated that an increase

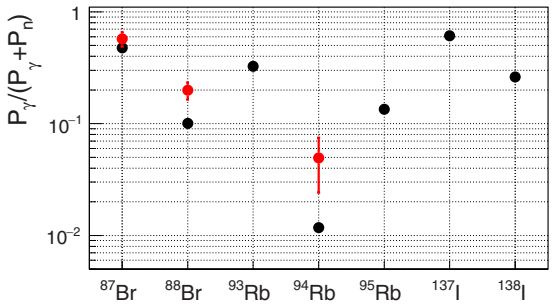

Figure 7. Integrated Γ-branching from states populated in the decay above the neutron separation energy. In black Hauser-Feschbach estimate, in red experimental results.

of $\langle\Gamma_\gamma\rangle$ by a factor of 20 will bring the $2J+1$ weighted average in agreement with the experiment. A decrease of $\langle\Gamma_n\rangle$ of the same magnitude will have a similar effect. It is not easy to reconcile the large renormalization needed for $\langle\Gamma_\gamma/\Gamma_{\rm tot}\rangle$ with our current understanding of the PSF and the OM. Further decay experiments for well chosen β-delayed neutron emitters are required to investigate this issue. Notice, however, that a renormalization of $\langle\Gamma_\gamma\rangle$ of such magnitude, if confirmed and generalized, will have a significant impact on (n, γ) cross section estimates.

We discuss now the possibility of using the result of HFF calculations to anticipate cases where the γ-branching can be expected to be large. The calculation of P_γ,

$$P_\gamma = \int_{S_n}^{Q_\beta} \sum_i w(J_i^\pi, E_x) \left\langle \frac{\Gamma_\gamma(J_i^\pi, E_x)}{\Gamma_{\rm tot}(J_i^\pi, E_x)} \right\rangle I_\beta(E_x) dE_x \tag{5}$$

requires a knowledge of the full β intensity distribution above S_n. If this information is missing, from experiment and theory, we will show that one can still obtain useful information using an approximate $I_\beta(E_x)$. We have found that in all the decays discussed here the β-intensity above S_n can be approximated, on average, by a constant β-strength function $S_\beta(E_x) = \text{const.}$,

$$I_\beta(E_x) = T_{1/2} f(Q_\beta - E_x) S_\beta(E_x) \tag{6}$$

i.e., an intensity proportional to the statistical Fermi rate function $f(Q_\beta - E_x)$. Other approximations, such as a β-strength proportional to the level density [25], could be used as well. Using the constant β-strength approximation we calculate the ratio $P_\gamma/(P_\gamma + P_n)$ for the cases we have studied as shown in Fig. 7. This ratio is independent of the normalization of $I_\beta(E_x)$.

In Fig. 7 we also show the experimental branchings that were published earlier [6,7]. We observe a good agreement for ^{87}Br and the disagreement already discussed for ^{94}Rb. For ^{88}Br the calculation can match the experiment if we assume that the weight w of 0^- states in the decay (see Table 1) is 20% instead of 11%, the $(2J+1)$ weight. The preliminary results for ^{93,95}Rb and ^{137}I, although not shown, agree well with the estimate. One can conclude that a simple approximation for the β intensity in combination with the HFF calculation provides a fair estimate of the γ branching from neutron unbound states populated in β decay.

5. Conclusion

Total absorption γ-ray spectroscopy was used to measure accurately the β-intensity populating states above the neutron separation energy that is followed by γ-ray emission for seven well known β-delayed neutron emitters. The ratio of the integrated intensity for γ emission to the total intensity is surprisingly large for most of the cases, ranging from 17% to 57%. These large branchings are compatible with Hauser-Feshbach calculations, showing that the common reason is the hindrance of neutron emission because of the large orbital angular momentum transfer required to populated the available levels in the final nucleus. This calls for a revision of the common assumption that γ emission is negligible in comparison to neutron emission from neutron unbound states populated in the decay. In one of the cases, ^{94}Rb, the γ-branching is only 5% as neutron emission from the states populated is not particularly hindered. However this value is much larger than the value obtained from Hauser-Feshbach calculations using standard statistical model parameters. The difference could be matched by increasing the ratio of the radiative width to the neutron width by a factor 20. It is difficult to accommodate an increase of this magnitude in our current understanding of photon strength functions and neutron transmission coefficients. However a large increase of the γ width, if confirmed and generalized, will have an impact on r process abundance calculations. Further work is needed to understand this issue and measurements on suitable new β-delayed neutron emitters are planned.

This work was supported by Spanish Ministerio de Economía y Competitividad under grants FPA2008-06419, FPA2010-17142, FPA2011-24553, FPA2014-52823-C2-1-P, CPAN CSD-2007-00042 (Ingenio2010) and the program Severo Ochoa (SEV-2014-0398). WG would like to thank the University of Valencia for support. This work was supported by the Academy of Finland under the Finnish Centre of Excellence Programme 2012-2017 (Project No. 21350). Work supported by EPSRC(UK) and STFC(UK) and the UK National Measurement Office. Work supported by the European Commission under the FP7/EURATOM contract 605203. FGK acknowledges support from the U.S. Department of Energy, under contract number DE-AC02-06CH11357.

References

[1] S. Goriely, Phys. Lett. B **436**, 10 (1998)
[2] R. Surman et al., Phys. Rev. C **64**, 035801 (2001)
[3] A. Arcones et al., Phys. Rev. C **83**, 045809 (2011)
[4] T. Rauscher et al., Atom. Data and Nucl. Data Tables **75**, 1 (2000)
[5] Evaluated Nuclear Structure Data File (ENSDF), `http://www.nndc.bnl.gov/ensdf/`
[6] J. L. Tain et al., Phys. Rev. Lett. **115**, 062502 (2015)
[7] E. Valencia et al., `arXiv:1609.06128 [nucl-ex]`, submitted to Phys. Rev. C
[8] J. L. Tain et al., Nucl. Instrum. Methods Phys. Res., Sect. A **774**, 17 (2015)
[9] J. L. Tain et al., Nucl. Instrum. Methods Phys. Res., Sect. A **803**, 36 (2015)
[10] V. Guadilla et al., Nucl. Instrum. Methods Phys. Res., Sect. B **376**, 334 (2016)

[11] I. Moore et al., Nucl. Instrum. Methods Phys. Res., Sect. B **317**, 208 (2013)
[12] T. Eronen et al., Eur. Phys. J. A **48**, 46 (2012)
[13] D. Cano-Ott et al., Nucl. Instrum. Methods Phys. Res., Sect. A **430**, 333 (1999)
[14] S. Agostinelli et al., Nucl. Instrum. Methods Phys. Res., Sect. A **506**, 250 (2003)
[15] J. L. Tain et al., Nucl. Instrum. Methods Phys. Res., Sect. A **571**, 728 (2007)
[16] RIPL-3, R. Capote et al., Nucl. Data Sheets **110**, 3107 (2009)
[17] S. Goriely et al., Phys. Rev. C **78**, 064307 (2008)
[18] A. J. Koning et al., Proceedings International Conference on Nuclear Data for Science and Technology, April 22–27, 2007, Nice, France, EDP Sciences (2008) 211
[19] A. J. Koning et al., Nucl. Phys. A **713**, 231 (2003)
[20] B. Jonson et al., Proc. 3rd Int. Conf. on Nuclei far from stability, CERN Report 76–13 (1976) 277
[21] J. L. Tain et al., Nucl. Instrum. Methods Phys. Res., Sect. A **571**, 719 (2007)
[22] T. Kawano and P. Talou, Nucl. Data Sheets **118**, 183 (2014)
[23] P. G. Hansen, Adv. Nucl. Phys. **7**, 159 (1973)
[24] M.B. Chadwick et al., Nucl. Data Sheets **112**, 2887 (2011)
[25] A. C. Pappas and T. Sverdrup, Nucl. Phys. A **188**, 48 (1972)